Title

Ceftriaxone ameliorates tau pathology and cognitive decline via restoration of glial glutamate transporter in a mouse model of Alzheimer's disease

Journal

Neurobiology of Aging, 36(7)

ISSN

01974580

Authors

Zumkehr, Joannee
Rodriguez-Ortiz, Carlos J
Cheng, David
et al.

Publication Date

2015-07-01

DOI

10.1016/j.neurobiolaging.2015.04.005

Peer reviewed

Neurobiology of Aging 36 (2015) 2260–2271

Contents lists available at ScienceDirect

Neurobiology of Aging

journal homepage: www.elsevier.com/locate/neuaging

Ceftriaxone ameliorates tau pathology and cognitive decline via restoration of glial glutamate transporter in a mouse model of Alzheimer's disease

Joannee Zumkehr [a], Carlos J. Rodriguez-Ortiz [a], David Cheng [b], Zanett Kieu [a], Thin Wai [a], Charlesice Hawkins [a], Jason Kilian [a], Siok Lam Lim [a], Rodrigo Medeiros [b], Masashi Kitazawa [a,*]

[a] Molecular and Cell Biology, School of Natural Sciences, University of California, Merced, Merced, CA, USA
[b] Department of Neurobiology and Behavior, University of California, Irvine, Irvine, CA, USA

ARTICLE INFO

Article history:
Received 15 January 2015
Received in revised form 24 March 2015
Accepted 8 April 2015
Available online 16 April 2015

Keywords:
Alzheimer's disease
Astrocyte
GLT-1
Tau
Amyloid β

ABSTRACT

Glial glutamate transporter, GLT-1, is the major Na^+-driven glutamate transporter to control glutamate levels in synapses and prevent glutamate-induced excitotoxicity implicated in neurodegenerative disorders including Alzheimer's disease (AD). Significant functional loss of GLT-1 has been reported to correlate well with synaptic degeneration and severity of cognitive impairment among AD patients, yet the underlying molecular mechanism and its pathological consequence in AD are not well understood. Here, we find the temporal decrease in GLT-1 levels in the hippocampus of the 3xTg-AD mouse model and that the pharmacological upregulation of GLT-1 significantly ameliorates the age-dependent pathological tau accumulation, restores synaptic proteins, and rescues cognitive decline with minimal effects on Aβ pathology. In primary neuron and astrocyte coculture, naturally secreted Aβ species significantly downregulate GLT-1 steady-state and expression levels. Taken together, our data strongly suggest that GLT-1 restoration is neuroprotective and Aβ-induced astrocyte dysfunction represented by a functional loss of GLT-1 may serve as one of the major pathological links between Aβ and tau pathology.

1. Introduction

Alzheimer's disease (AD) is the most common progressive neurodegenerative disease associated with dementia. Neuropathological hallmarks include extracellular amyloid-beta (Aβ) plaques and intracellular neurofibrillary tangles (NFTs) composed of Aβ peptides and hyperphosphorylated tau proteins, respectively. Buildup of these pathological lesions are believed to trigger complex, multifactorial neurodegenerative cascades in AD leading to synaptic loss and neurodegeneration. Dementia severity among AD patients correlates well with synaptic loss and oligomeric Aβ species and to a lesser extent, with Aβ plaques in the brain (Dickson et al., 1992; Haass and Selkoe, 2007; Hardy and Selkoe, 2002; Scheff et al., 2006; Selkoe, 2002; Tomic et al., 2009). Moreover, increasing Aβ levels has been suggested to be an initiating factor in AD pathology (Haass and Selkoe, 2007). The exact molecular mechanism that links Aβ and tau pathology in AD, however, remains largely unknown.

Clinical and preclinical evidence suggests disruption of glutamate homeostasis contributes to the development of neuropathological hallmarks and cognitive decline in AD. Glutamate neurotransmission is critically involved in learning and memory, and its synapses are densely concentrated in the hippocampus, a vulnerable region affected in AD. Its neurotransmission is tightly controlled by 5 different glutamate transporters within the vicinity of glutamatergic synapses in humans to prevent prolonged glutamate input and subsequent glutamate-induced excitotoxicity in neurons. Among these transporters, the excitatory amino acid transporter 2 or its mouse homologue glutamate transporter 1 (GLT-1, herein collectively referred to as GLT-1) expressed predominantly on astrocytes is responsible for regulating 90% of glutamate levels in the synapses (Kim et al., 2011). A significant reduction of GLT-1 activity has been reported to occur in an early stage of AD and correlates well with synaptic loss and cognitive decline in patients (Masliah et al., 1996). In addition, GLT-1 gene expression and protein levels are altered in the hippocampus of AD patients (Jacob et al., 2007). Recent studies further support the

* Corresponding author at: Department of Molecular and Cell Biology, School of Natural Sciences, University of California, Merced, 5200 North Lake Road, Merced, CA 95343, USA. Tel.: 209 228 4164; fax: 209-228-4060.
E-mail address: mkitazawa@ucmerced.edu (M. Kitazawa).

0197-4580/$ – see front matter
http://dx.doi.org/10.1016/j.neurobiolaging.2015.04.005

involvement of GLT-1 in AD by showing that the heterozygous knockdown of GLT-1 in an AD mouse model exacerbates cognitive decline without affecting Aβ pathology and that astrocytic GLT-1 dysfunction plays an important role in human AD pathogenesis (Mookherjee et al., 2011; Woltjer et al., 2010). These studies evidently show that impairment in GLT-1 is not only part of the initial stages of AD pathology but that it also plays an important role in the progression of cognitive decline.

In this study, we investigate whether compensation for the age- and pathology-dependent loss of GLT-1 would significantly impact AD-like neuropathology and cognitive decline in the triple transgenic mouse model of AD (3xTg-AD). We hypothesize that a loss of GLT-1, representative of functional impairments of astrocytes, mediates Aβ-induced neurotoxicity and precedes postsynaptic degeneration and cognitive decline in AD, and its restoration rescues functional synapses and halts the disease progression. Here, we show that the chronic upregulation of GLT-1 by ceftriaxone significantly attenuates tau pathology, restores synaptic proteins, and rescues cognition without affecting Aβ pathology in 3xTg-AD mice. Our in vitro studies uncover that naturally secreted Aβ species significantly downregulate GLT-1 expression. Taken together, loss of GLT-1 may in part mediate Aβ-triggered tau pathology in AD.

2. Materials and methods

2.1. Animals

All experiments were carried out in accordance with the Institutional Animal Care and Use Committee at the University of California and were consistent with Federal guidelines. All mice were housed on a 12-hour light-dark schedule with ad libitum access to food and water. The 3xTg-AD mice express the Swedish (K670N/M671L), $PS1_{M146V}$, and tau (P301L; found in frontotemporal dementia patients) mutations which increase the overall production of Aβ, increases the ratio of $Aβ_{42}/Aβ_{40}$ and promotes tau tangle formation, respectively (Oddo et al., 2003b). A total of 5–7 3xTg-AD mice and 5–7 strain-matched C57BL6/129SvJ nontransgenic mice were used for the aging study. A total of 15 3xTg-AD mice were treated; 4 females and 4 males for the vehicle group and 3 females and 4 males for the ceftriaxone-treated group.

2.2. Animal treatment paradigm

Ten-month-old 3xTg-AD mice were treated intraperitoneally (i.p.) with 200 mg/kg ceftriaxone (Santa Cruz Biotechnology, Santa Cruz, CA, USA) or 0.8% sodium chloride (Vehicle) daily for 2 months (Rothstein et al., 2005). On completion of the treatment period and cognitive evaluation, mice were anesthetized and perfused with ice-cold phosphate-buffered saline and brains were collected. One hemisphere of the brain was fixed with 4% paraformaldehyde for immunostaining. The other hemisphere was microdissected into the hippocampus and cortex. The hippocampus was homogenized in T-PER buffer containing protease and phosphatase inhibitors followed by the centrifugation at 100,000*g* for 1 hour to separate the detergent-soluble fraction and insoluble pellets. Pellets were subsequently homogenized in 70% formic acid and the detergent-insoluble fractions were collected. Samples were stored at −80 °C until further analysis.

2.3. Cognitive tests

After the 2 months of ceftriaxone treatment, all mice were subjected to cognitive evaluation in the Morris water maze (MWM) and novel object recognition test (NOR). As described previously (Kitazawa et al., 2011), the apparatus used for the MWM task was a circular aluminum tank (1.2-m diameter) painted white and filled with water maintained at 22–24 °C. The maze was located in a room containing several simple visual extramaze cues. Mice were trained to swim and find a 14-cm diameter circular clear Plexiglas platform submerged 1.5 cm beneath the surface of the water and invisible to the mice while swimming. On each training trial, mice were placed into the tank at 1 of 4 designated start points in a pseudorandom order. Mice were allowed to find and escape onto the platform. If mice failed to find the platform within 60 seconds, they were manually guided to the platform and allowed to remain there for 10 seconds. Each day, mice received 4 training sessions separated by intervals of 25 seconds under a warming lamp. The training period ended when all groups of mice reached criterion (<25 seconds mean escape latency). The probe trial to examine retention memory was assessed 24 hours after the last training trial. In the probe trials, the platform was removed from the pool, and mice were monitored by a ceiling-mounted camera directly above the pool during the 1-minute period. All trials were recorded for subsequent analysis. The parameters measured during the probe trial included: (1) latency to cross the platform location and (2) number of platform location crosses.

The NOR was performed as described previously (Blurton-Jones et al., 2009). Briefly, mice were habituated in the test environment for 3 days (5 minutes per day). In the acquisition of familiar objects, mice were exposed to 2 identical objects separated in a specific location in a square cage. Twenty-four hours later, mice were placed in the test cage with 1 familiar object and 1 novel object. The total amount of time the mice explored each object was recorded separately for 3 minutes, and the recognition index ([time spent on novel object]/[{time to spent on novel object} + {time spent on a familiar object}]) was calculated in %.

2.4. Quantitative Aβ enzyme-linked immunosorbent assay analysis

Soluble and insoluble $Aβ_{1\text{-}40}$ and $Aβ_{1\text{-}42}$ levels were measured by enzyme-linked immunosorbent assay (ELISA) as previously described (Kitazawa et al., 2011). Briefly, 96-well plates (Immulon 2HB, Fisher Scientific, Waltham, MA, USA) were coated with 25 μg/mL of the mouse anti-Aβ monoclonal antibody (clone 20.1) in carbonate coating buffer pH 9.6 (Sigma-Aldrich, St. Louis, MO, USA) and incubated overnight at 4 °C. The wells were washed and blocked with 3% bovine serum albumin (BSA) overnight at 4 °C with shaking. After washing, serial dilutions of $Aβ_{40}$ and $Aβ_{42}$ were added to the wells and plates were sealed then incubated overnight at 4 °C with shaking. After washing, horseradish peroxidase–conjugated affinity anti-$Aβ_{40}$ or anti-$Aβ_{42}$ antibodies were added at 1:2000 and 1:1000 dilutions, respectively, and incubated overnight at 4 °C with shaking. Wells were then washed and incubated with streptavidin–horseradish peroxidase (1:4000 dilution) for 4 hours at room temperature, washed then Ultra-TMB ELISA substrate (Pierce, Rockford, IL, USA) was added for 5–10 minutes to develop the reaction. The reaction was stopped by adding 2N H_2PO_4 and plates were analyzed on a SpectraMax spectrophotometer (Molecular Devices, Sunnyvale, CA, USA) at 450 nm. The plasma end-point titer was defined as the maximal plasma dilution in which the optical density for the antibodies was 3 times higher than the optical density values of the blank wells.

2.5. Western blot analysis

Protein concentrations of detergent-soluble fractions from half brain (hippocampus or cortex) were determined by the Bradford protein assay. These fractions (9 μg of protein) were subsequently immunoblotted with the following antibodies: HT7 (total human tau; Pierce Biotechnology), AT8 (phosphorylated tau at S202/T205; Pierce Biotechnology), PHF-1 (phosphorylated tau at S396/S404; a

kind gift from Dr. Peter Davies, Albert Einstein College of Medicine), CP13 (phosphorylated at S202/T205; a kind gift from Dr. Peter Davies, Albert Einstein College of Medicine), AT100 (phosphorylated tau at S212/T214, Pierce Biotechnology), GLT-1 (a kind gift from Dr. Jeffrey David Rothstein, Johns Hopkins University), glial fibrillary acidic protein (GFAP) (Dako, Carpinteria, CA, USA), cdk5 (Calbiochem, La Jolla, CA, USA), p35/p25 (Santa Cruz Biotechnology), GSK-3β (BD transduction laboratories, San Jose, CA, USA), and phospho-GSK-3β (phosphorylation at S9, Cell Signaling Technology, Beverly, MA, USA). Glyceraldehyde-3-phosphate dehydrogenase (GAPDH), (Santa Cruz Biotechnology), tubulin and/or actin (Abcam, Cambridge, MA, USA) were used to control for protein loading or to confirm no cross-contamination of each fraction. Band intensity was measured using the Odyssey Image station and Image Studio (version 2.1, LI-COR Biosciences, Lincoln, NE, USA) and normalized by corresponding loading control proteins.

2.6. Real-time polymerase chain reaction

Total RNA was isolated from 3xTg-AD or wild-type (WT) hippocampal tissue using TRI reagent (Molecular Research Center, Cincinnati, OH, USA). Total RNA was isolated from untreated and treated neuron and astrocyte primary cells using Direct-zol RNA MiniPrep (ZYMO RESEARCH Corp, Irvine, CA, USA). Briefly, 1 μg of total RNA was used for one-cycle reverse transcriptase reaction to make complementary DNA by random hexamers using 5× iScript reaction mix and iScript reverse transcriptase (Bio-Rad, Hercules, CA, USA). Two microliters of resulting complementary DNA was subjected to a PCR reaction for the detection of GLT-1, glutamate aspartate transporter (GLAST), and GFAP using Power SYBR Green PCR Master Mix (Applied Biosystems, Life-Technologies). Sequences of GLT-1 primers were 5′-TTCCAAGCCTGGATCACT GCTC-3′ (forward) and 5′-GGACGAATCTGGTCACACGCTT-3′ (reverse) (Origene, NM_001077514). GLAST primers were 5′-GCGATTGG TCGCGGTGATAATG-3′ (forward) and 5′-CGACAATGACTGTCACGGTGTAC-3′ (reverse) (Origene, NM_148938). GFAP primers were 5′-CACCTACAGGAAATTGCTGGAGG-3′ (forward) and 5′-CCACGATGTTCCTCTTGAGGTG-3′ (reverse) (Origene, NM_010277). GAPDH was used for normalizing the GLT-1, GLAST, and GFAP expression levels in each treatment, and the primer sequences were 5′-AACTTTGGCATTGTGGAAGG-3′ and 5′- ACACATTGGGGGTAGGAACA-3′. The PCR cycle parameters were as follows: denaturing step (95 °C for 15 seconds), annealing step (60 °C for 60 seconds), and extension step (72 °C for 30 seconds). The cycle threshold (Ct) values were determined by SDS Software v1.3.1 (Applied Biosystems), and ΔCt for each treatment group was calculated as follows: ΔCt = Ct (GLT-1, GLAST1, or GFAP) - Ct (GAPDH) (Langmann et al., 2006).

2.7. Immunohistochemical and immunofluorescence staining

Each half brain was cut into 20-μm slices using a microtome and stored in phosphate-buffered saline with 0.05% sodium azide. Free-floating sections were washed with tris-buffered saline (TBS), permeablized with 0.1% triton X-100, and blocked with 3% BSA in TBS. For Aβ plaque burden and certain tau staining, free-floating sections were pretreated with 90% formic acid for 3 minutes before the incubation with primary antibodies. Sections were then incubated with antibodies against synaptophysin (SYP; presynaptic marker; Abcam; 1:1000), postsynaptic density protein 95 kDa (PSD95; postsynaptic marker; NeuroMab; 1:1000), AT8 (1:2000), AT100 (1:2000), CP13 (1:1000), PHF1 (1:1000), MC1 (1:1000), HT7 (1:2000), Iba-1 (1:400), 4G8 (1:400), or biotinylated antibody against $A\beta_{42}$ (clone D32 from Drs. Vasilevko and Cribbs, 1:400) overnight. Sections were washed the following day and incubated with 3% BSA and 1% triton X-100 in TBS then incubated for 1 hour with corresponding secondary antibody conjugated with Alexa Fluor 488, Alexa Fluor 555, and/or Alexa Fluor 633 with 4′,6-diamidino-2-phenylindole for nuclear staining. For immunohistochemistry, after the incubation with primary antibodies, sections were incubated with corresponding biotinylated secondary antibodies, followed by avidin-biotin complex treatment and 3, 3′-diaminobenzidine staining according to the manufacturer's specifications.

2.8. Thioflavin S staining

For immunofluorescent staining with thioflavin S (Sigma), free-floating sections were mounted on a SuperFrost Plus microscope slide (Fisher Scientific) to dry overnight. To hydrate, fixed sections were immersed twice in 100% ethanol for 2 minutes, twice in 95% ethanol for 2 minutes, once in 70% ethanol for 2 minutes, and then once in 50% ethanol for 2 minutes. Sections were then incubated with 0.5% thioflavin S in 50% ethanol for 10 minutes (in the dark). Sections were washed twice with 50% ethanol for 3 minutes and twice with water for 3 minutes. Staining was visualized using a digital inverted microscope (EVOS-fl, Advanced Microscopy Group).

2.9. Quantitative analysis of synaptic proteins, plaque burden, and tau pathology

Synapse proteins in the CA1 and CA3 regions of the hippocampus and dentate gyrus (DG) were quantified by ImageJ software. Briefly, 6 brain sections (20-μm thickness) from each animal were immunofluorescence (IF) stained with SYP or PSD95 antibodies described previously and images were captured using a digital inverted microscope (EVOS-fl, Advanced Microscopy Group). PSD95 or SYP IF signal were counted in the subfield of the hippocampus and DG. SYP and PSD95 protein levels were calculated independently. For each 20-μm brain section, 3 different areas from the CA1 and CA3 regions of the hippocampus and DG were captured. From those images, 3 random 100-μm^2 sections were chosen (each representative of that area) from each image and the mean intensity was measured using ImageJ software. An average of all the areas from each region was calculated and represented synapse intensity for DG, CA1, or CA3 of the hippocampus. Staining with 4G8, HT7, or PHF-1 was also analyzed in the same manner. For the CP13, HT7, and PHF-1 analysis, the entire area of the hippocampus and cortex (separately) was chosen of 2–5 brain sections (20-μm thickness) and positive soma were counted from each area.

2.10. Astrocyte and neuron primary cell coculture

As described by Yang et al. (2009), primary astrocytes were extracted from the cortex and hippocampus of postnatal day 2–3 (P2–P3) mice from WT mice. Primary cells were grown in Dulbecco's Modified Eagle's Medium containing 10% fetal bovine serum (FBS) and 1% penicillin or streptomycin (P or S). Primary neurons were extracted from embryonic day 14–16 (E14–16) of WT mice. Primary neurons were added to confluent primary astrocytes in Neurobasal media with B27 supplement, glutamine, and 5% FBS (plating media) for the first 24 hours then the medium was changed to media of similar contents but with only 2.5% FBS (growth media). Primary cells were treated after day 7 (of neuron addition) (Yang et al., 2009). The purity of primary astrocytes and the presence of neurons were consistently monitored by IF staining with GFAP and tau5, respectively.

2.11. 7PA2–Chinese hamster ovary (CHO) cell culture

Naturally secreted Aβ monomers and oligomers were obtained from the conditioned medium (CM) of 7PA2–Chinese hamster ovary (CHO) cells that express the V717F AD mutation in amyloid

precursor protein (APP_{751}) (an APP isoform, i.e., 751 amino acids in length, a kind gift from Dr. Edward Koo, UCSD) (Walsh et al., 2002). Both control CHO cells and 7PA2 cells were grown in the Dulbecco's Modified Eagle's Medium containing 10% FBS and 1% P or S until ~90% confluency. Cells were washed and medium replaced with neuronal growth media (described previously) for ~18 hours. CM was collected and centrifuged at 1000*g* for 10 minutes at 4 °C to remove cell debris and then used for treatment of astrocyte and neuron primary cell coculture. CM from CHO cells and fresh growth media were used as controls.

2.12. Statistical analysis

All immunoblot and immunohistochemical data were quantitatively analyzed using Image Studio (version 2.1) software or ImageJ software. Statistics were carried out using 1-way analysis of varaince with post hoc tests or unpaired *t* test and $p < 0.05$ or lower was considered to be significant. Pearson correlation coefficient was calculated for linear regression graphs.

3. Results

To determine whether the expression of GLT-1 in astrocytes changed with age and/or the progression of the AD-like pathological hallmarks in 3xTg-AD mouse model, we assessed levels of GLT-1 in the hippocampus from 2–3 (prepathological), 6 (early pathology), 12–13 (mild and/or moderate pathology), or 23 (late, established pathology) months of age. We found that the hippocampal GLT-1 expression and the steady-state levels significantly decreased as AD-like neuropathology progressed in 3xTg-AD mice but not in WT mice ($p < 0.05$ and $p < 0.01$; Fig. 1A, C, and D). The steady-state levels of GLT-1 were significantly reduced especially at 12 months of age or older. We previously reported that GFAP steady-state levels increase with age in 3xTg-AD mice (Oddo et al., 2003a). In this study, we found that GFAP messenger RNA expression levels as well as the steady-state levels also increased with age in 3xTg-AD mice ($p < 0.01$; Fig. 1B, C, and F). Thus astrogliosis inversely correlated with significant GLT-1 decrease indicating that glial GLT-1 in synapses was less in the 3xTg-AD mice than that in

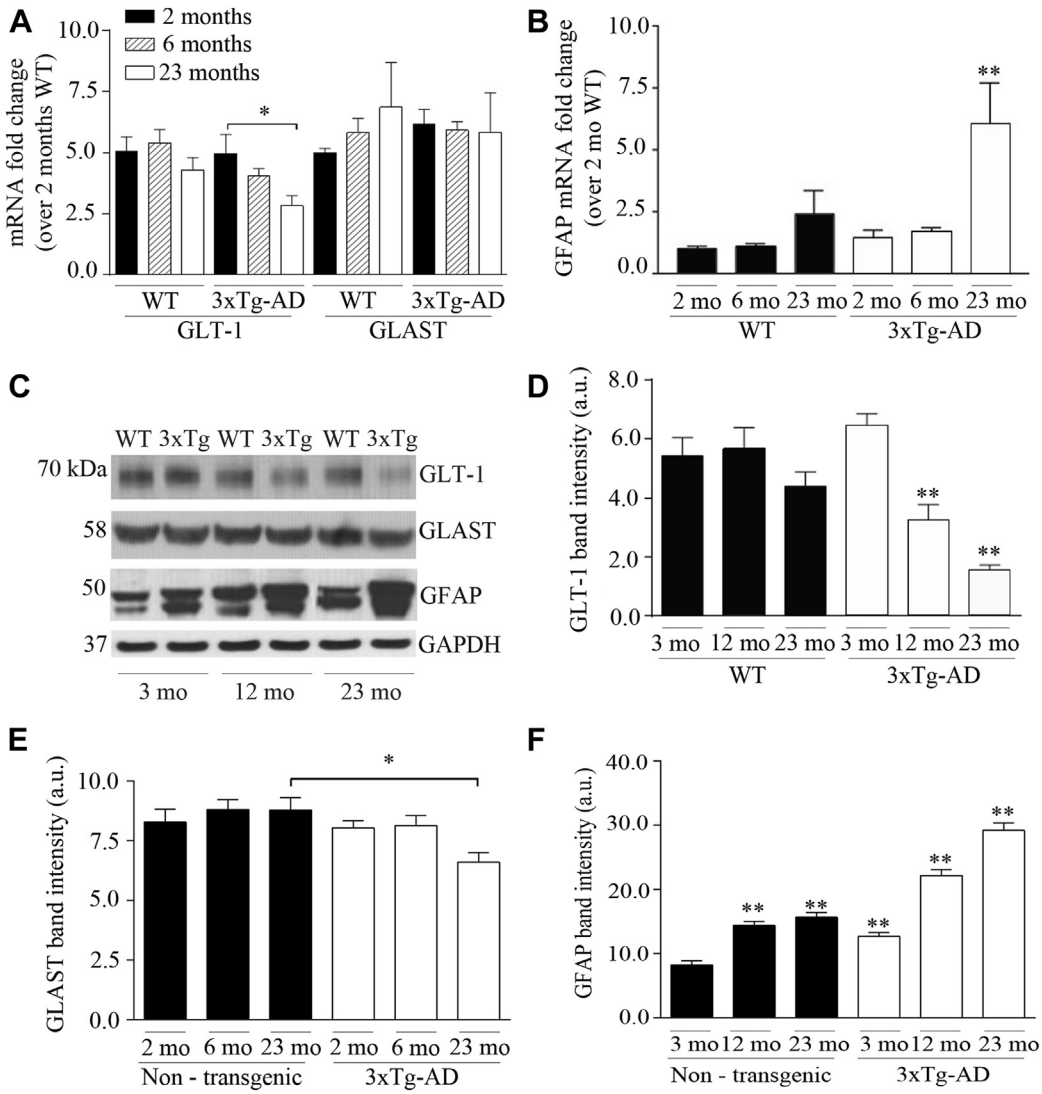

Fig. 1. GLT-1 decreases in an age-dependent manner in 3xTg-AD mice. (A) Real-time polymerase chain reaction analysis (RT-PCR) of GLT-1 mRNA levels in wild-type (WT) and 3xTg-AD mice at 2, 6, and 23 months (mo) old mice. (B) RT-PCR analysis of GFAP mRNA levels in WT and 3xTg-AD 2-, 6-, and 23-month-old mice. (C) Western blot analysis of protein extracts from 3-, 12-, and 23-month-old WT and 3xTg-AD mice using GLT-1, GFAP, and GAPDH antibodies. The densitometric analysis of the GLT-1 (D), GLAST (E), and GFAP (F) bands normalized to GAPDH shown in the graphs. Each bar is expressed as mean ± standard error mean; $^{*}p < 0.05$ and $^{**}p < 0.01$ compared with the WT group or 2- to 3-month-old 3xTg-AD group. The number of mice analyzed was n = 5–7 per group. Abbreviations: AD, Alzheimer's disease; GFAP, glial fibrillary acidic protein; GLAST, glutamate aspartate transporter; GLT-1, glutamate transporter 1; mRNA, messenger RNA.

age-matched WT mice. In comparison, the GLAST expression and steady-state levels, also expressed on astrocytes, did not significantly decrease until 23 months of age ($p < 0.05$ Fig. 1C and E).

Recent studies have demonstrated that synthetic oligomeric $A\beta_{1-42}$ decreased GLT-1 expression or promoted mislocalization of GLT-1 from the cell surface of primary astrocytes, leading to glutamate dyshomeostasis in synapses (Abdul et al., 2009; Scimemi et al., 2013). Our in vivo evidence (Fig. 1), however, indicated a clear reduction of GLT-1; a reduction possibly through the decreased expression in astrocytes. To test whether Aβ species subsequently alters GLT-1 expression, we used the primary neuron and astrocyte co-culture system to examine the role of naturally secreted Aβ species on GLT-1 expression in vitro (Yang et al., 2009); 1.85 nM of naturally secreted $A\beta_{42}$ and 4.4 nM of naturally secreted $A\beta_{40}$ in the CM from 7PA2 CHO cells (7PA2-CM) (Walsh et al., 2002) were added to primary neuron and/or astrocyte coculture for 48 hours (Fig. 2A). We found that the 48-hour treatment of 7PA2-CM resulted in a significant decrease of the GLT-1 messenger RNA expression ($p < 0.0001$ Fig. 2B) compared with cells treated with CM from CHO cells (CHO-CM; control). GLAST expression did not change under the same treatment (Fig. 2B, right). We also investigated the steady levels of GLT-1 and found that Aβ species from the 7PA2-CM significantly decreased the steady-state levels compared with CHO-CM ($p < 0.0001$ Fig. 2C). Integrity of primary astrocyte and

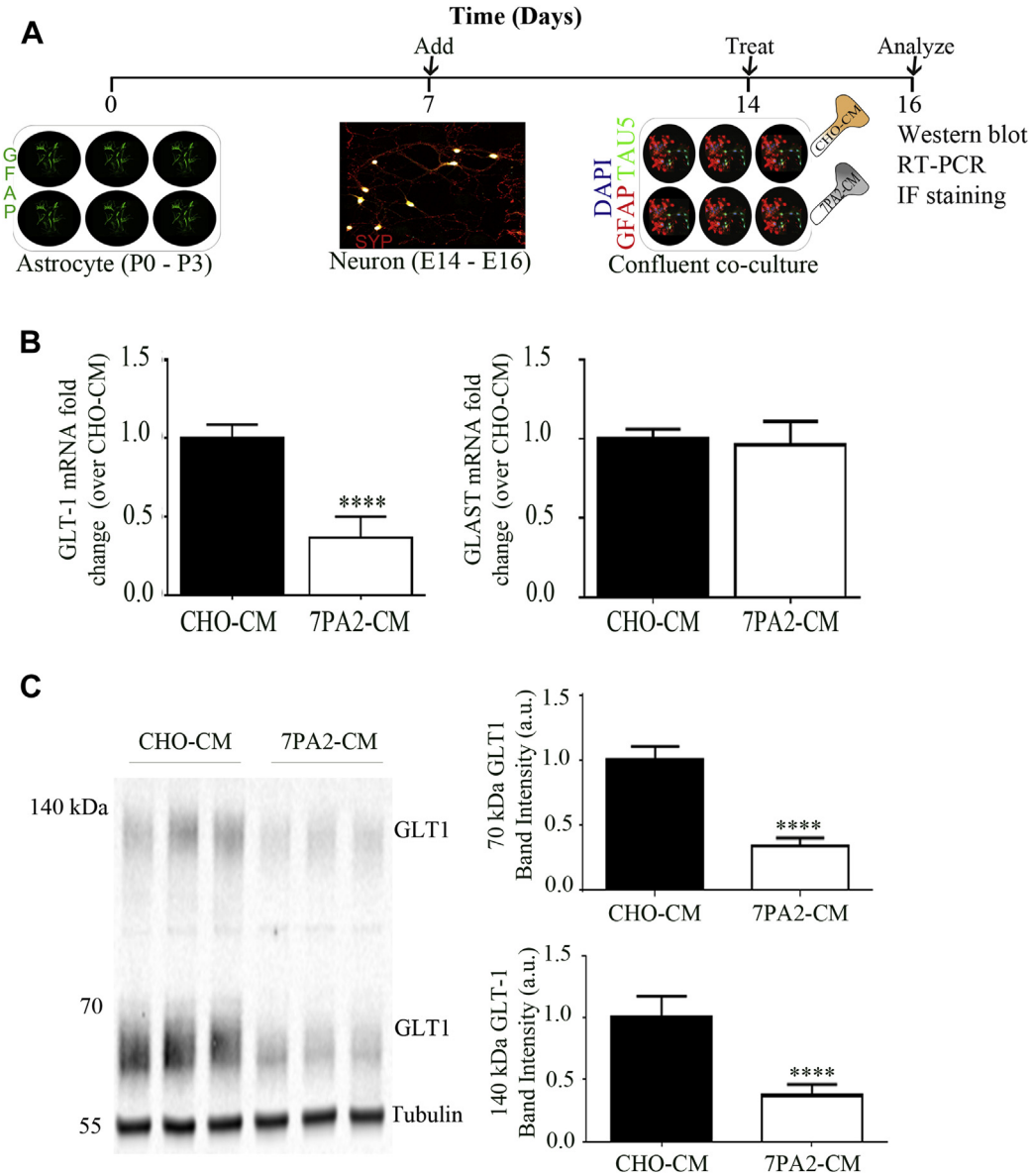

Fig. 2. Naturally secreted amyloid-beta (Aβ) decrease GLT-1 steady state levels. (A) Experimental scheme for investigating GLT-1 expression in the primary astrocyte and neuron coculture. Astrocytes extracted from the cortex and hippocampus of postnatal day 0–3 (P0–P3) and detected with the GFAP antibody. Neurons were extracted from embryonic day 14–16 (E14–E16) and detected with tau5 or SYP antibodies; 1.85 nM of naturally secreted $A\beta_{42}$ and 4.4 nM of naturally secreted $A\beta_{40}$ present in 7PA2-CM (quantified by enzyme-linked immunosorbent assay) were added to the coculture for 48 hours. (B) RT-PCR analysis of GLT-1 and GLAST mRNA levels from neuron and astrocyte cocultures treated with CHO-conditioned media (CHO-CM) or 7PA2-conditioned media (7PA2-CM) for 48 hours. (C) Western blot of protein extracts from neuron and astrocyte cocultures treated with 7PA2-CM or CHO-CM for 48 hours using GLT-1 and tubulin antibodies. The densitometric analysis of the 70 kDa and 140 kDa band from GLT shown in the graph. Each bar is expressed as mean ± standard error of the mean; $^{****}p < 0.0001$ 7PA2-CM compared with CHO-CM. Three independent experiments performed each time in triplicates. Abbreviations: CHO, Chinese hamster ovary; GFAP, glial fibrillary acidic protein; GLAST, glutamate aspartate transporter; GLT-1, glutamate transporter 1; IF, immunofluorescence; mRNA, messenger RNA; RT-PCR, real-time polymerase chain reaction; SYP, synaptophysin.

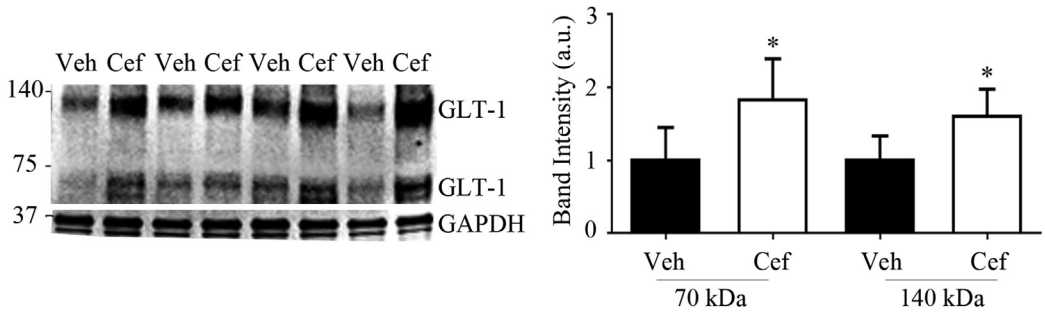

Fig. 3. Chronic ceftriaxone-treatment increases GLT-1 expression levels in 3xTg-Alzheimer's disease (AD) mice. Western blot analysis of protein extracts from hippocampal tissue of 12-month-old 3xTg-AD mice using GLT-1 and GAPDH (housekeeping) antibodies. Densitometric analysis of the GLT-1 bands normalized to GAPDH shown in the graph. Each bar is expressed as mean ± standard error of the mean; $^{*}p < 0.05$, ceftriaxone-treated 3xTg-AD mice compared with the vehicle-treated 3xTg-AD mice (n = 5 mice per group). Molecular weight markers are in kDa. Abbreviations: Cef, ceftriaxone treatment; GLT-1, glutamate transporter 1; Veh, vehicle or saline-treatment.

neuron cocultures was consistently confirmed through IF staining (Fig. 2A). These in vitro results suggest that Aβ species are responsible for the loss of GLT-1 expression as a part of their toxicity to astrocytes.

Because a significant reduction of GLT-1 was evident in the hippocampus of 3xTg-AD mice at 12 months of age and our in vitro evidence suggested that its reduction was mediated by Aβ species, we examined whether a chronic restoration of GLT-1 at this age would ameliorate downstream AD-like neuropathology and cognitive decline. We chronically treated 10-month-old 3xTg-AD mice with either ceftriaxone (200 mg/kg i.p.) or saline (0.8% NaCl i.p.) daily for 2 months. Ceftriaxone is a beta lactam antibiotic shown to increase the astroglial GLT-1 expression both in vitro and in vivo (Lee et al., 2008; Rothstein et al., 2005). Consistent with these previous reports, the ceftriaxone treatment in this study significantly increased GLT-1 protein expression levels compared with the age-matched vehicle group ($p < 0.05$ for both 70 and 140 kDa bands; Fig. 3). GLT-1 Western blots can show monomeric (70 kDa) and dimeric (140 kDa) forms as previously shown and described (Danbolt, 2001; Rothstein et al., 2005).

The effect of GLT-1 upregulation on hippocampal-dependent cognition was evaluated by MWM and NOR immediately after treatment. During the acquisition training in the MWM, the vehicle 3xTg-AD group were capable of learning within the same day, but failed to retain spatial memory from day to day, which was consistent with previous findings (Billings et al., 2005). In comparison, the ceftriaxone-treated 3xTg-AD group had better retention for most of the training days ($p < 0.05$; Fig. 4A). This was later confirmed during the probe trial of MWM; the probe trial measures retention memory. During the probe trial, the ceftriaxone-treated group reached the platform location significantly faster than the vehicle group ($p < 0.05$; Fig. 4B). In addition, ceftriaxone-treated mice crossed the platform location more than the vehicle group within the 60 seconds of the probe trial, further suggesting that the

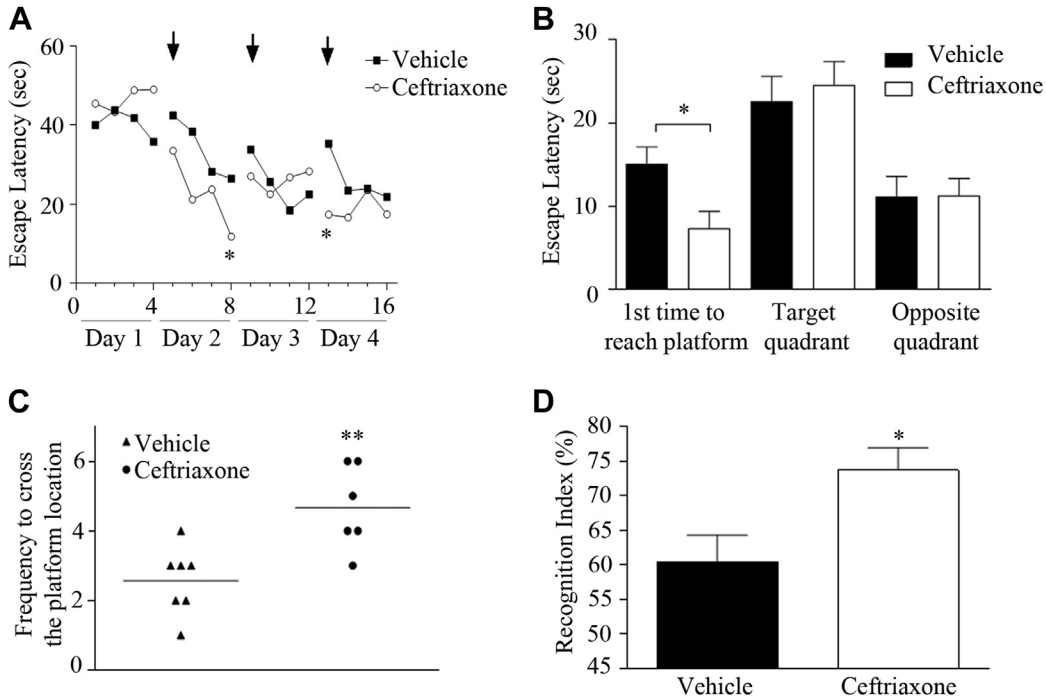

Fig. 4. Upregulation of GLT-1 by ceftriaxone ameliorates cognitive decline in 3xTg-AD mice. (A) Acquisition curve during training of Morris water maze (MWM) expressed as average of all mice in each group. Arrowheads show the first training of the day. (B) Escape latency and (C) number of crosses on platform location for 24-hour retention trial in MWM. (D) Novel object recognition test for the first minute of the test. Each bar is expressed as mean ± standard error of the mean; $^{*}p < 0.05$ and $^{**}p < 0.01$, ceftriaxone-treated 3xTg-AD mice compared with the vehicle-treated 3xTg-AD mice (n = 5 mice per group). Abbreviation: GLT-1, glutamate transporter 1.

retention memory was significantly rescued in the ceftriaxone-treated mice ($p < 0.01$; Fig. 4C). Similarly, in the NOR, ceftriaxone-treated mice explored a novel object significantly longer than a familiar object ($p < 0.05$; Fig. 4D). Therefore, increasing GLT-1 in the 3xTg-AD mice rescued cognitive impairments as measured by 2 independent behavioral tests.

To better understand the molecular basis of the restoration of cognition in these behavioral tests, we examined the effects of GLT-1 upregulation on Aβ and tau pathology. Quantitative ELISA revealed no significant changes of detergent-insoluble $A\beta_{40}$ and $A\beta_{42}$ in the hippocampal tissues of 3xTg-AD mice (Fig. 5A). Detergent-soluble $A\beta_{40}$ significantly ($p < 0.01$; Fig. 5A) increased in

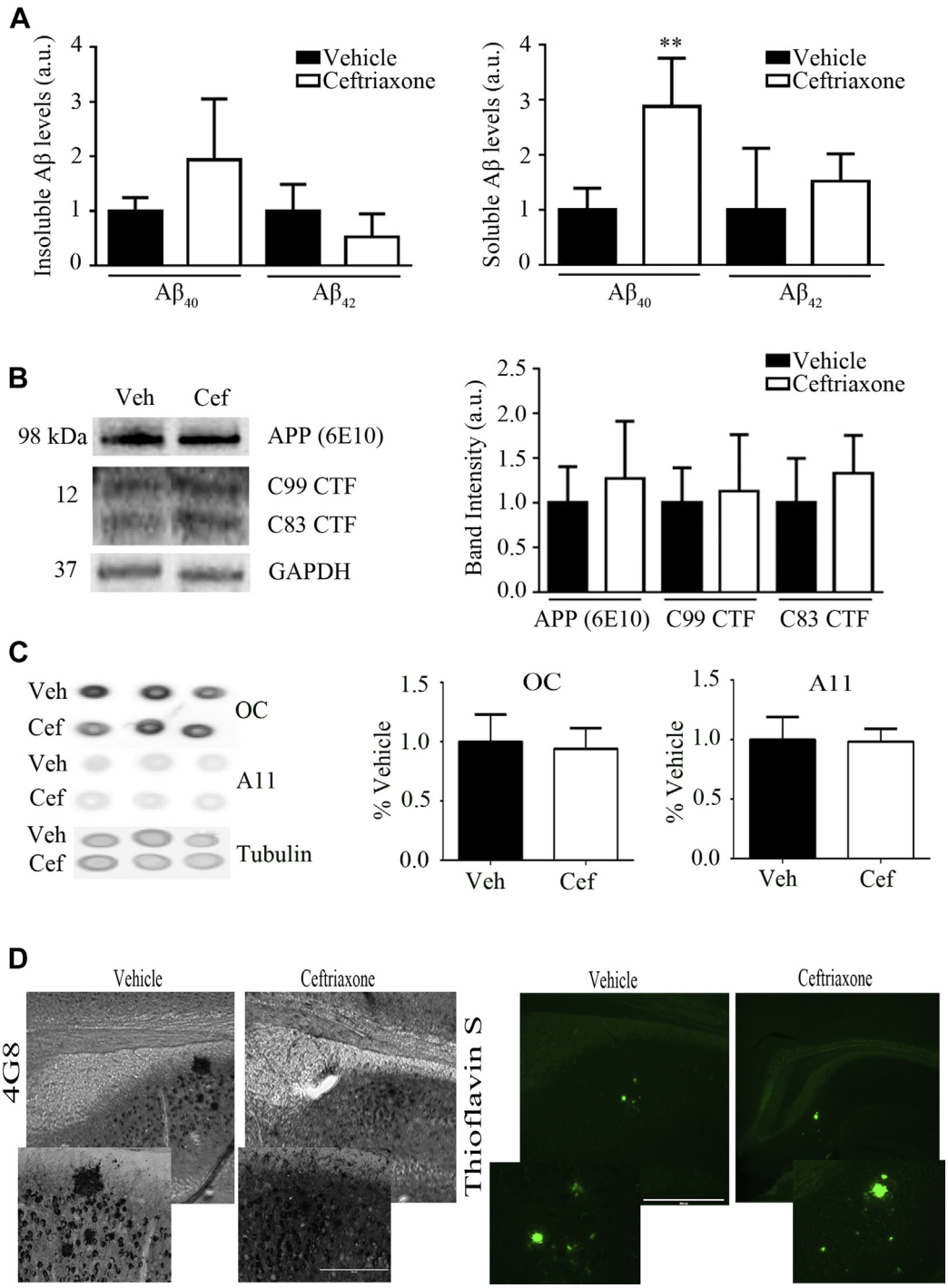

Fig. 5. Effect of GLT-1 upregulation on Aβ pathology in 3xTg-AD mice. (A) Quantitative Aβ ezyme-linked immunosorbent assay in detergent-insoluble (formic acid soluble) brain hippocampal fraction and detergent-soluble brain hippocampal fraction. (B) Western blot analysis of APP processing in the hippocampus of the brain. The densitometric analysis of C99 and C83 fragments shown in the graph. (C) Dot blot analysis of soluble prefibrillar and fibrillar Aβ oligomers in the cortical soluble fractions detected by the A11 and OC antibodies respectively. (D) Qualitative representation of the immunohistochemical staining with 4G8 and thioflavin S to detect Aβ plaques. Each bar is expressed in mean ± standard error of the mean; $^{**}p < 0.01$, ceftriaxone-treated 3xTg-AD mice compared with the vehicle-treated 3xTg-AD mice (n = 4–5 mice per group). Abbreviations: Aβ, amyloid-beta; AD, Alzheimer's disease; Cef, ceftriaxone; GLT-1, glutamate transporter 1; Veh, vehicle.

ceftriaxone-treated mice; however, there was no significance in detergent-soluble $A\beta_{42}$ (Fig. 5A). APP expression or processing was not significantly altered by the treatment because the steady-state levels of APP or C-terminal fragments of APP, specifically C99 and C83, were not changed among the treatment groups (Fig. 5B). We then used conformation-specific antibodies, A11 and OC, to detect soluble prefibrillar and fibrillar Aβ oligomers, respectively (Kayed et al., 2003, 2007). Dot blot analysis of the cortical soluble fractions revealed no significant changes in Aβ oligomer levels between the ceftriaxone-treated and vehicle-treated 3xTg-AD mice (Fig. 5C). Together with our in vitro data above, the presence of Aβ species likely suppressed GLT-1 expression in the brain of 3xTg-AD mouse. In addition, histological analysis revealed that plaque burden in the hippocampus and subiculum of ceftriaxone-treated 3xTg-AD mice were not significantly different than the vehicle group, which in part supported the quantitative ELISA data described previously (Fig. 5D). Although we do not know the exact mechanisms of increased soluble $A\beta_{40}$ levels in the ceftriaxone-treated mice, collectively, these results suggest that GLT-1 dysfunction does not affect APP processing, overall Aβ species levels, and plaque pathology in the 3xTg-AD mice. These findings are consistent with a recent report in heterozygous knockout of GLT-1 in APP/PS1 mice (Mookherjee et al., 2011).

We previously demonstrated that altered inflammation such as gliosis in the brain exacerbated tau pathology in 3xTg-AD mice (Kitazawa et al., 2005, 2011). Accordingly we investigated pathological changes in tau after upregulation of GLT-1. Histopathological analysis revealed that the ceftriaxone-treated mice showed significantly less CP13-positive tau (pSer202) bearing neurons than vehicle-treated mice in the cortex and hippocampus ($p < 0.05$;

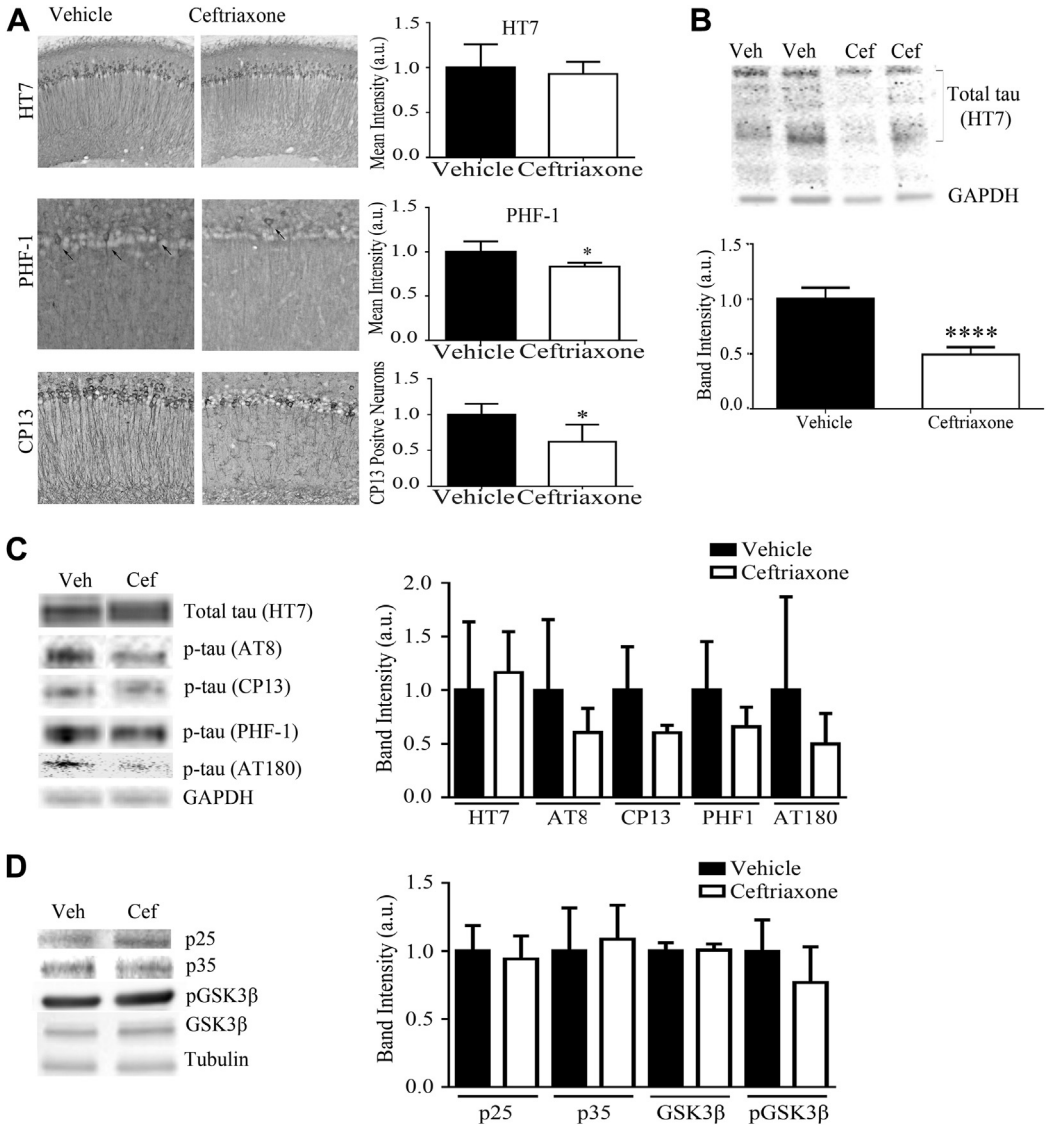

Fig. 6. Effect of GLT-1 upregulation on tau pathology in 3xTg-AD mice. (A) Representative Immunohistochemical or immunofluorescence staining with tau antibodies HT7, PHF-1, and CP13 antibodies. The mean intensities of HT7 and PHF-1 from immunofluorescence staining are shown in the graph along with the CP13 positive neuron analysis. Arrows point to tau-positive neurons. (B) Representative Western blot image of total human tau using HT7 antibody from the sarkosyl–insoluble cortical protein fraction. The densitometric analysis of all bands are shown in the graph. (C) Western blot analysis of total human tau using HT7 antibody and various phosphor-specific tau using PHF1, AT8, CP13, AT180, and GAPDH (housekeeping protein) from the detergent-soluble hippocampal protein fraction. The densitometric analysis of PHF1, AT8, CP13 and AT180 are shown in the graph. (D) Western blot analysis of known tau kinases: p25, p35, phosphor-GSK3β (pGSK3β), GSK3β, and tubulin (housekeeping protein) on detergent-soluble hippocampal protein fraction. The densitometric analysis of p25, p35, phosphor-GSK3β, and GSK3β are shown in the graph. Each bar is expressed as mean ± standard error of the mean; $^{*}p < 0.05$, ceftriaxone-treated 3xTg-AD mice compared with the vehicle-treated 3xTg-AD mice (n = 4–5 mice per group); $^{****}p < 0.0001$. Abbreviations: AD, Alzheimer's disease; Cef, ceftriaxone; GLT-1, glutamate transporter 1; Veh, vehicle.

Fig. 6A). Similarly, the mean intensity from IF staining with the PHF-1 antibody (pSer396/Ser404) was significantly less than the vehicle group in the CA1 region of the hippocampus ($p < 0.05$; Fig. 6A). No significant alteration in total tau levels by the HT7 antibody was detected in the same fields. Western blot analysis of the insoluble total tau levels in sarkosyl-insoluble fraction of the cortex was significantly lower in the ceftriaxone-treated 3xTg-AD mice ($p < 0.0001$; Fig. 6B). Western blot analysis of tau in detergent-soluble fraction of hippocampus showed a decreasing trend, though not significant, of phospho-specific tau using the PHF-1, AT8, CP13, and AT180 antibodies while the total tau levels remained unchanged (Fig. 6C). This discrepancy suggests decreased levels of insoluble or aggregated tau in the hippocampus of ceftriaxone-treated 3xTg-AD mice. We investigated the kinases reported in the involvement of pathological tau phosphorylation (Dhavan and Tsai, 2001; Götz and Ittner, 2008). Although we found a decreasing trend of phosphor-specific tau, the total steady-state levels of cdk5 and GSK-3β were not significantly altered among the treatment groups (Fig. 6D). Taken together, these results highlights disease-modifying effects of GLT-1 on tau pathology in neurons.

3xTg-AD mice display an age-dependent dramatic loss of synapses without extensive neuronal loss (Blurton-Jones et al., 2009; LaFerla and Oddo, 2005). Therefore, we examined whether a restoration of GLT-1 protected synaptic proteins in these mice. Synapse alterations were quantitatively analyzed by changes in synaptic markers SYP (Dickson et al., 1995; Masliah, 2000; Sze et al., 1997; Terry et al., 1991) and PSD95 (Zhao et al., 2006). Significant changes of SYP and PSD95 immunoreactivity in subregions within hippocampus were observed by IF staining (Fig. 7A–B). Quantitative analysis of fluorescent signals revealed that synaptic proteins detected by the SYP and PSD95 antibodies was significantly preserved in the CA3 region of the hippocampus ($p < 0.05$; Fig. 7A–B) of ceftriaxone-treated 3xTg-AD mice. In addition, a significant restoration of PSD95 immunoreactivity in CA1 hippocampus was also observed in the ceftriaxone-treated 3xTg-AD mice ($p < 0.001$ and $p < 0.05$; Fig. 7B). We also found the restoration of PSD95 had a tendency to correlate with augmented cognitive performance by MWM. Mice reaching the platform in 15 seconds or less had a high (>1.0) synaptic protein intensity mean, and although not statistically significant, increased PSD95 mean fluorescent intensity negatively correlated with the escape latency in DG, CA1, and CA3 regions of hippocampus (Fig. 7C). These findings strongly indicate that GLT-1 is the key to preserving synapses and crucial for neuron to neuron communication.

4. Discussion

We report that astrocytic GLT-1 may be a key player that links Aβ and tau pathology. Our findings show a significant correlation between the age-dependent decrease of astrocytic GLT-1 and the progression of AD-like neuropathology in 3xTg-AD mice regardless of astrogliosis. To test whether the loss of GLT-1 precede AD

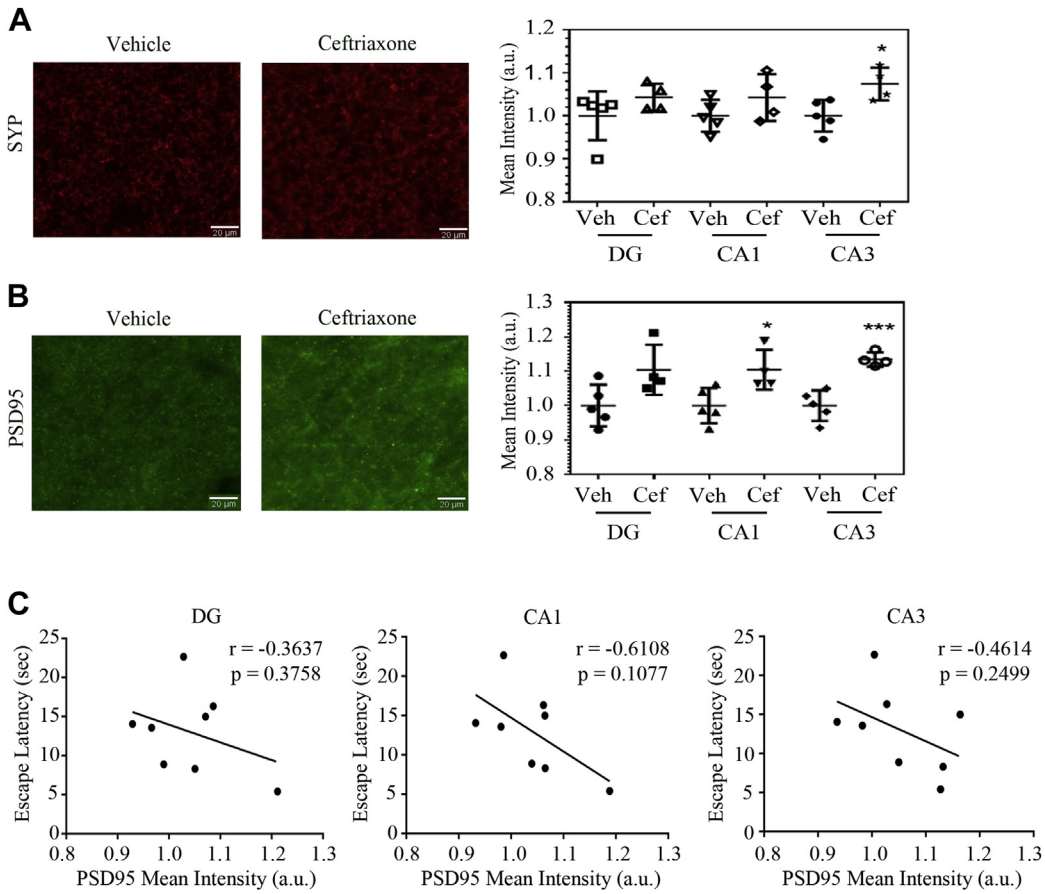

Fig. 7. Synaptic proteins restored in ceftriaxone-treated 3xTg-Alzheimer's disease (AD) mice. (A) Representative immunofluorescence (IF) images of SYP in the CA3 region of the hippocampus and quantitative analysis of the average mean intensities from 5 IF (20 μm) stained sections in the dentate gyrus (DG), CA1, and CA3 of the hippocampus. (B) Representative IF images of PSD95 in the CA3 region of the hippocampus and quantitative analysis of the average mean intensities from 5 IF (20 μm) stained sections in the DG, CA1, and CA3 of the hippocampus. (C) Escape latency as a function of synaptic protein mean intensity graphs in the designated region of the hippocampus. Each shape represents 1 mouse and each bar is expressed as mean ± standard error of the mean; $^{*}p < 0.05$ and $^{***}p < 0.001$, ceftriaxone-treated 3xTg-AD mice compared with the vehicle-treated 3xTg-AD mice (n = 3–5 mice per group). Abbreviations: Cef, ceftriaxone; PSD95, postsynaptic density protein 95 kDa; sec, seconds; SYP, synaptophysin; Veh, vehicle.

pathology and cognitive decline in 3xTg-AD mice, we pharmacologically overexpressed GLT-1 and examined its pathological and behavioral consequences in vivo. By doing so, we found that the chronic administration of ceftriaxone significantly increases GLT-1 expression, ameliorates cognitive deficits, preserves synaptic proteins, and decreases tau pathology in aged 3xTg-AD mice. These results strongly implicate and support the notion that astrocyte dysfunction have major implications in neurodegenerative disease particularly AD. Furthermore, alteration of glutamate transporter expression occurs in the early stages of AD human patients—an important factor in finding a cure (Masliah et al., 1996).

Synaptic density significantly decreases in human AD brains (Scheff et al., 2006; Terry et al., 1991) and AD mouse model brains (Mucke et al., 2000; Oddo et al., 2003b). Along with this, increasing evidence shows the active involvement of astrocytes in synapse formation, function, and elimination (Clarke and Barres, 2013). Talantova et al. in particular showed the involvement of astrocytes in glutamate-induced synaptic damage via α-7 nicotinic receptors stimulation and extrasynaptic N-methyl-d-aspartate–type glutamate receptors (Talantova et al., 2013). In comparison, our study focuses on glutamate regulation via GLT-1 expression. We show a positive and significant correlation between an increase in GLT-1 steady-state levels and synaptic proteins (PSD95 and SYP). In particular, a restoration of PSD95 is more evident and found in DG, CA1, and CA3 regions of hippocampus after ceftriaxone treatment, indicating a beneficial effect of GLT-1 in postsynaptic neurons. These results further support our hypothesis that the loss of GLT-1 triggers excitotoxicity and degeneration of postsynaptic neurons through aberrant calcium influx. Restoration of synaptic glutamate homeostasis attenuates postsynaptic degeneration more significantly and directly than presynapses. These changes in part contribute to the restoration of cognitive function in the ceftriaxone-treated 3xTg-AD mice as shown by the correlation curve (Fig. 7C).

As previous studies indicate, Aβ species can induce toxicity to cells before plaque formation and synaptic loss (Cleary et al., 2004; Li et al., 2009; Mucke et al., 2000; Townsend et al., 2006; Walsh et al., 2002). In addition to those studies, we propose that Aβ species also induce astrocyte dysfunction that affect pathology progression in AD. Our results clearly show that Aβ species (including monomers and oligomers) downregulate GLT-1 expression in vitro and that GLT-1 restoration in vivo did not affect soluble Aβ species levels (Figs. 2 and 5). Although GLT-1 is predominantly expressed on astrocytes, neurons also express GLT-1 (Chen et al., 2002, 2004). Thus, further studies are needed to investigate the contribution of neuronal GLT-1 expression. Nonetheless, Aβ-induced GLT-1 dysfunction may occur in the early stages of AD. This effect can lead to glutamate dyshomeostasis and/or glutamate excitotoxicity. This phenomenon has been suggested in AD because AD patients have increasing glutamate levels in their cerebral spinal fluid as dementia progresses (Jimenez-Jimenez et al., 1998; Kaiser et al., 2010).

GLT-1 downregulation also has important implications on tau propagation, phosphorylation, and dephosphorylation as perturbation of this equilibrium can void tau's microtubule-associated function, lead to aberrant tau aggregates, and increase neuron vulnerability in AD. Because GLT-1 indirectly affect calcium level influx, its dysfunction can impact tau calcium-dependent kinases, including GSK-3β and cdk5 and induce NFTs (Blurton-Jones and LaFerla, 2006; Dhavan and Tsai, 2001; Götz and Ittner, 2008). Additionally, an increase in calcium influx can lead to an increase in calcium-dependent tau interneuronal propagation (Pooler et al., 2013). Studies have also shown that tau can spread synaptically via connected glutamatergic neurons (de Calignon et al., 2012; Liu et al., 2012). This presents the possibility that glutamate dyshomeostasis can be one of the driving forces of tau pathology.

NFTs correlate with cognitive decline (Giannakopoulos et al., 2003) and are initiated by the abnormal accumulation and mislocalization of tau in somatodendritic compartments. Tau can also facilitate Fyn kinase to postsynaptic compartments whereby Fyn phosphorylates one of the N-methyl-D-aspartate receptor (NMDAR) subunits, NR2b, thereby stabilizing its interaction with PSD95 thus causing a sustained activation of NMDAR (Ittner et al., 2010). Our study, however, showed no significant alterations in the NR2b subunit in the ceftriaxone-treated mice (data not shown). In addition GSK-3β and p25 were not significantly different in the ceftriaxone-treated 3xTg-AD mice. Overall, GLT-1 overexpression ameliorated tau pathology and cognition which suggests that GLT-1 is critical for AD progression.

The nuclear factor kappa B pathway is involved in ceftriaxone-induced GLT1 expression; ceftriaxone increases the nuclear factor kappa B binding to the GLT-1 promoter thus increasing its expression (Lee et al., 2008). Ceftriaxone has also been shown to transport through the blood-brain barrier (Spector, 1987). Previous reports have shown that ceftriaxone impairs hippocampal learning and memory in rats or had no effect in mice (Karaman et al., 2013; Matos-Ocasio et al., 2014). Our study investigates the AD model while Matos-Ocasio et al. (2014) and Karaman et al. (2013) investigated WT animal models. Opposite results may suggest adverse effects in normal conditions. As stated by Matos-Ocasio et al. (2014), GLT1 overexpression may be detrimental to normal neuronal activity. In addition, our study chronically injected ceftriaxone for 2 months whereas the other 2 studies treated for only 8–9 days. Thus duration of ceftriaxone treatment may be crucial in improving learning and memory.

5. Conclusion

In conclusion, our study elucidates the involvement of the glial glutamate transporter in the pathogenesis of AD. We propose that Aβ species before plaque or fibrillar formation initiate GLT-1 downregulation in the early stages of AD. This accounts for the progressive decrease in GLT-1 expression seen in 3xTg-AD, unaffected progression of Aβ pathology, and how the 7PA2 conditioned media containing Aβ species decreased the steady-state levels of GLT-1 in vitro. We also propose that Aβ-induced GLT-1 dysfunction mediates downstream AD neuropathology including synaptic loss and tau pathology. Further studies, however, are needed to show underlying molecular mechanisms by which Aβ affects GLT-1 downregulation and alteration in vivo. Although further studies will also be needed to confirm any confounding variables from the pharmacological approach, this study determined an important role of astrocyte dysfunction in AD. Moreover, we find that the restoration of GLT-1 ameliorates tau pathology and cognitive deficits. Our study raises the possibility that targeting GLT-1 may result in disease-modifying therapies for not only AD, but also other neurodegenerative disorders, such as tauopathies.

Disclosure statement

The authors have no conflicts of interest to disclose.

Acknowledgements

The authors thank Dr. J. Rothstein (Johns Hopkins University) and Dr. P. Davies (Albert Einstein College of Medicine) for generously providing us antibodies used in this study. The authors also thank Dr. Y. Yang (Tufts University) for sharing experimental techniques and technical comments. This project is funded by the Alzheimer's Association Grant, NIRG-12-242598 (Masashi Kitazawa).

References

Abdul, H.M., Sama, M.A., Furman, J.L., Mathis, D.M., Beckett, T.L., Weidner, A.M., Patel, E.S., Baig, I., Murphy, M.P., LeVine, H., Kraner, S.D., Norris, C.M., 2009. Cognitive decline in Alzheimer's disease is associated with selective changes in calcineurin/NFAT signaling. J. Neurosci. 29, 12957–12969.

Billings, L.M., Oddo, S., Green, K.N., McGaugh, J.L., LaFerla, F.M., 2005. Intraneuronal Aβ causes the onset of early Alzheimer's disease-related cognitive deficits in transgenic mice. Neuron 45, 675–688.

Blurton-Jones, M., Kitazawa, M., Martinez-Coria, H., Castello, N.A., Müller, F.-J., Loring, J.F., Yamasaki, T.R., Poon, W.W., Green, K.N., LaFerla, F.M., 2009. Neural stem cells improve cognition via BDNF in a transgenic model of Alzheimer disease. Proc. Natl. Acad. Sci. U. S. A. 106, 13594–13599.

Blurton-Jones, M., LaFerla, F.M., 2006. Pathways by which A facilitates tau pathology. Curr Alzheimer Res 3, 437–448.

Chen, W., Aoki, C., Mahadomrongkul, V., Gruber, C.E., Wang, G.J., Blitzblau, R., Irwin, N., Rosenberg, P.A., 2002. Expression of a variant form of the glutamate transporter GLT1 in neuronal cultures and in neurons and astrocytes in the rat brain. J. Neurosci. 22, 2142–2152.

Chen, W., Mahadomrongkul, V., Berger, U.V., Bassan, M., DeSilva, T., Tanaka, K., Irwin, N., Aoki, C., Rosenberg, P.A., 2004. The glutamate transporter GLT1a is expressed in excitatory axon terminals of mature hippocampal neurons. J. Neurosci. 24, 1136–1148.

Clarke, L.E., Barres, B.A., 2013. Emerging roles of astrocytes in neural circuit development. Nat. Rev. Neurosci. 14, 311–321.

Cleary, J.P., Walsh, D.M., Hofmeister, J.J., Shankar, G.M., Kuskowski, M.A., Selkoe, D.J., Ashe, K.H., 2004. Natural oligomers of the amyloid-β protein specifically disrupt cognitive function. Nat. Neurosci. 8, 79–84.

Danbolt, N.C., 2001. Glutamate uptake. Prog. Neurobiol. 65, 1–105.

de Calignon, A., Polydoro, M., Suárez-Calvet, M., William, C., Adamowicz, David H., Kopeikina, Kathy J., Pitstick, R., Sahara, N., Ashe, Karen H., Carlson, George A., Spires-Jones, Tara L., Hyman, Bradley T., 2012. Propagation of tau pathology in a model of early Alzheimer's disease. Neuron 73, 685–697.

Dhavan, R., Tsai, L., 2001. A decade of CDK5. Nat. Rev. Mol. Cell Biol. 2, 10.

Dickson, D.W., Crystal, H.A., Bevona, C., Honer, W., Vincent, I., Davies, P., 1995. Correlations of synaptic and pathological markers with cognition of the elderly. Neurobiol. Aging 16, 285–298.

Dickson, D.W., Crystal, H.A., Mattiace, L.A., Masur, D.M., Blau, A.D., Davies, P., Yen, S.-H., Aronson, M.K., 1992. Identification of normal and pathological aging in prospectively studied nondemented elderly humans. Neurobiol. Aging 13, 179–189.

Giannakopoulos, P., Herrmann, F.R., Bussière, T., Bouras, C., Kövari, E., Perl, D.P., Morrison, J.H., Gold, G., Hof, P.R., 2003. Tangle and neuron numbers, but not amyloid load, predict cognitive status in Alzheimer's disease. Neurology 60, 1495–5000.

Götz, J., Ittner, L.M., 2008. Animal models of Alzheimer's disease and frontotemporal dementia. Nat. Rev. Neurosci. 9, 532–544.

Haass, C., Selkoe, D.J., 2007. Soluble protein oligomers in neurodegeneration: lessons from the Alzheimer's amyloid β-peptide. Nat. Rev. Mol. Cell Biol. 8, 101–112.

Hardy, J., Selkoe, D.J., 2002. The amyloid hypothesis of Alzheimer's disease: progress and problems on the road to therapeutics. Science 297, 353–356.

Ittner, L.M., Ke, Y.D., Delerue, F., Bi, M., Gladbach, A., van Eersel, J., Wölfing, H., Chieng, B.C., Christie, M.J., Napier, I.A., 2010. Dendritic function of tau mediates amyloid-β toxicity in Alzheimer's disease mouse models. Cell 142, 387–397.

Jacob, C., Koutsilieri, E., Bartl, J., Neuen-Jacob, E., Arzberger, T., Zander, N., Ravid, R., Roggendorf, W., Riederer, P., Grünblatt, E., 2007. Alterations in expression of glutamatergic transporters and receptors in sporadic Alzheimer's disease. J. Alzheimers Dis. 11, 97–116.

Jimenez-Jimenez, F., Molina, J., Gomez, P., Vargas, C., De Bustos, F., Benito-Leon, J., Tallon-Barranco, A., Orti-Pareja, M., Gasalla, T., Arenas, J., 1998. Neurotransmitter amino acids in cerebrospinal fluid of patients with Alzheimer's disease. J. Neural Transm. 105, 269–277.

Kaiser, E., Schoenknecht, P., Kassner, S., Hildebrandt, W., Kinscherf, R., Schroeder, J., 2010. Cerebrospinal fluid concentrations of functionally important amino acids and metabolic compounds in patients with mild cognitive impairment and Alzheimer's disease. Neurodegener. Dis. 7, 251–259.

Karaman, I., Kizilay-Ozfidan, G., Karadag, C.H., Ulugol, A., 2013. Lack of effect of ceftriaxone, a GLT-1 transporter activator, on spatial memory in mice. Pharmacol. Biochem. Behav. 108, 61–65.

Kayed, R., Head, E., Sarsoza, F., Saing, T., Cotman, C.W., Necula, M., Margol, L., Wu, J., Breydo, L., Thompson, J.L., Rasool, S., Gurlo, T., Butler, P., Glabe, C.G., 2007. Fibril specific, conformation dependent antibodies recognize a generic epitope common to amyloid fibrils and fibrillar oligomers that is absent in prefibrillar oligomers. Mol. Neurodegener. 2, 18.

Kayed, R., Head, E., Thompson, J.L., McIntire, T.M., Milton, S.C., Cotman, C.W., Glabel, C.G., 2003. Common structure of soluble amyloid oligomers implies common mechanism of pathogenesis. Science 300, 486–489.

Kim, K., Lee, S.G., Kegelman, T.P., Su, Z.Z., Das, S.K., Dash, R., Dasgupta, S., Barral, P.M., Hedvat, M., Diaz, P., 2011. Role of excitatory amino acid transporter-2 (EAAT2) and glutamate in neurodegeneration: opportunities for developing novel therapeutics. J. Cell. Physiol. 226, 2484–2493.

Kitazawa, M., Cheng, D., Tsukamoto, M.R., Koike, M.A., Wes, P.D., Vasilevko, V., Cribbs, D.H., LaFerla, F.M., 2011. Blocking IL-1 signaling rescues cognition, attenuates tau pathology, and restores neuronal β-catenin pathway function in an Alzheimer's disease model. J. Immunol. 187, 6539–6549.

Kitazawa, M., Oddo, S., Yamasaki, T.R., Green, K.N., LaFerla, F.M., 2005. Lipopolysaccharide-induced inflammation exacerbates tau pathology by a cyclin-dependent kinase 5-mediated pathway in a transgenic model of Alzheimer's disease. J. Neurosci. 25, 8843–8853.

LaFerla, F.M., Oddo, S., 2005. Alzheimer's disease: Aβ, tau and synaptic dysfunction. Trends Mol. Med. 11, 170–176.

Langmann, T., Mauerer, R., Schmitz, G., 2006. Human ATP-binding cassette transporter TaqMan low-density array: analysis of macrophage differentiation and foam cell formation. Clin. Chem. 52, 310–313.

Lee, S.-G., Su, Z.-Z., Emdad, L., Gupta, P., Sarkar, D., Borjabad, A., Volsky, D.J., Fisher, P.B., 2008. Mechanism of ceftriaxone induction of excitatory amino acid transporter-2 expression and glutamate uptake in primary human astrocytes. J. Biol. Chem. 283, 13116–13123.

Li, S., Hong, S., Shepardson, N.E., Walsh, D.M., Shankar, G.M., Selkoe, D., 2009. Soluble oligomers of amyloid β protein facilitate hippocampal long-term depression by disrupting neuronal glutamate uptake. Neuron 62, 788–801.

Liu, L., Drouet, V., Wu, J.W., Witter, M.P., Small, S.A., Clelland, C., Duff, K., 2012. Trans-synaptic spread of tau pathology *In Vivo*. PLoS One 7, e31302.

Masliah, E., 2000. The role of synaptic proteins in Alzheimer's disease. Ann. N. Y. Acad. Sci. 924, 68–75.

Masliah, E., Hansen, L., Alford, M., Deteresa, R., Mallory, M., 1996. Deficient glutamate tranport is associated with neurodegeneration in Alzheimer's disease. Ann. Neurol. 40, 759–766.

Matos-Ocasio, F., Hernández-López, A., Thompson, K.J., 2014. Ceftriaxone, a GLT-1 transporter activator, disrupts hippocampal learning in rats. Pharmacol. Biochem. Behav. 122, 118–121.

Mookherjee, P., Green, P.S., Watson, G.S., Marques, M.A., Tanaka, K., Meeker, K.D., Meabon, J.S., Li, N., Zhu, P., Olson, V.G., 2011. GLT-1 loss accelerates cognitive deficit onset in an Alzheimer's disease animal model. J. Alzheimers Dis. 26, 447–455.

Mucke, L., Masliah, E., Yu, G.-Q., Mallory, M., Rockenstein, E.M., Tatsuno, G., Hu, K., Kholodenko, D., Johnson-Wood, K., McConlogue, L., 2000. High-level neuronal expression of Aβ1–42 in wild-type human amyloid protein precursor transgenic mice: synaptotoxicity without plaque formation. J. Neurosci 20, 4050–4058.

Oddo, S., Caccamo, A., Kitazawa, M., Tseng, B.P., LaFerla, F.M., 2003a. Amyloid deposition precedes tangle formation in a triple transgenic model of Alzheimer's disease. Neurobiol. Aging 24, 1063–1070.

Oddo, S., Caccamo, A., Shepherd, J.D., Murphy, M.P., Golde, T.E., Kayed, R., Metherate, R., Mattson, M.P., Akbari, Y., LaFerla, F.M., 2003b. Triple-transgenic model of Alzheimer's disease with plaques and tangles: intracellular Aβ and synaptic dysfunction. Neuron 39, 409–421.

Pooler, A.M., Phillips, E.C., Lau, D.H.W., Noble, W., Hanger, D.P., 2013. Physiological release of endogenous tau is stimulated by neuronal activity. EMBO Rep. 14, 389–394.

Rothstein, J.D., Patel, S., Regan, M.R., Haenggeli, C., Huang, Y.H., Bergles, D.E., Jin, L., Hoberg, M.D., Vidensky, S., Chung, D.S., 2005. β-Lactam antibiotics offer neuroprotection by increasing glutamate transporter expression. Nature 433, 73–77.

Scheff, S.W., Price, D.A., Schmitt, F.A., Mufson, E.J., 2006. Hippocampal synaptic loss in early Alzheimer's disease and mild cognitive impairment. Neurobiol. Aging 27, 1372–1384.

Scimemi, A., Meabon, J.S., Woltjer, R.L., Sullivan, J.M., Diamond, J.S., Cook, D.G., 2013. Amyloid-β1–42 slows clearance of synaptically released glutamate by mislocalizing astrocytic GLT-1. J. Neurosci. 33, 5312–5318.

Selkoe, D.J., 2002. Alzheimer's disease is a synaptic failure. Science 298, 789–791.

Spector, R., 1987. Ceftriaxone transport through the blood-brain barrier. J. Infect. Dis. 156, 209–211.

Sze, C.-I., Troncoso, J.C., Kawas, C., Moution, P., Price, D.L., Martin, L.J., 1997. Loss of the presynaptic vesicle protein synaptophysin in hippocampus correlates with cognitive decline in Alzheimer disease. J. Neuropathol. Exp. Neurol. 56, 933–944.

Talantova, M., Sanz-Blasco, S., Zhang, X., Xia, P., Akhtar, M.W., Okamoto, S.-i., Dziewczapolski, G., Nakamura, T., Cao, G., Pratt, A.E., Kang, Y.-J., Tu, S., Molokanova, E., McKercher, S.R., Hires, S.A., Sason, H., Stouffer, D.G., Buczynski, M.W., Solomon, J.P., Michael, S., Powers, E.T., Kelly, J.W., Roberts, A., Tong, G., Fang-Newmeyer, T., Parker, J., Holland, E.A., Zhang, D., Nakanishi, N., Chen, H.-S.V., Wolosker, H., Wang, Y., Parsons, L.H., Ambasudhan, R., Masliah, E., Heinemann, S.F., Piña-Crespo, J.C., Lipton, S.A., 2013. Aβ induces astrocytic glutamate release, extrasynaptic NMDA receptor activation, and synaptic loss. Proc. Natl. Acad. Sci. U. S. A. 110, E2518–E2527.

Terry, R.D., Masliah, E., Salmon, D.P., Butters, N., DeTeresa, R., Hill, R., Hansen, L.A., Katzman, R., 1991. Physical basis of cognitive alterations in Alzheimer's disease: synapse loss is the major correlate of cognitive impairment. Ann. Neurol. 30, 572–580.

Tomic, J.L., Pensalfini, A., Head, E., Glabe, C.G., 2009. Soluble fibrillar oligomer levels are elevated in Alzheimer's disease brain and correlate with cognitive dysfunction. Neurobiol. Dis. 35, 352–358.

Townsend, M., Shankar, G.M., Mehta, T., Walsh, D.M., Selkoe, D.J., 2006. Effects of secreted oligomers of amyloid β-protein on hippocampal synaptic plasticity: a potent role for trimers. J. Physiol. 572, 477–492.

Walsh, D.M., Klyubin, I., Fadeeva, J.V., Cullen, W.K., Anwyl, R., Wolfe, M.S., Rowan, M.J., Selkoe, D.J., 2002. Naturally secreted oligomers of amyloid β protein potently inhibit hippocampal long-term potentiation in vivo. Nature 416, 535–539.

Woltjer, R.L., Duerson, K., Fullmer, J.M., Mookherjee, P., Ryan, A.M., Montine, T.J., Kaye, J.A., Quinn, J.F., Silbert, L., Erten-Lyons, D., 2010. Aberrant detergent-insoluble excitatory amino acid transporter 2 accumulates in Alzheimer disease. J. Neuropathol. Exp. Neurol. 69, 667.

Yang, Y., Gozen, O., Watkins, A., Lorenzini, I., Lepore, A., Gao, Y., Vidensky, S., Brennan, J., Poulsen, D., Won Park, J., Li Jeon, N., Robinson, M.B., Rothstein, J.D., 2009. Presynaptic regulation of astroglial excitatory neurotransmitter transporter GLT1. Neuron 61, 880–894.

Zhao, L., Ma, Q.-L., Calon, F., Harris-White, M.E., Yang, F., Lim, G.P., Morihara, T., Ubeda, O.J., Ambegaokar, S., Hansen, J.E., 2006. Role of p21-activated kinase pathway defects in the cognitive deficits of Alzheimer disease. Nat. Neurosci. 9, 234–242.